

ZEKE Spectroscopy and Theoretical Calculations of Copper–Methylamine Complexes

Jun Miyawaki* and Ko-ichi Sugawara

Nanotechnology Research Institute, National Institute of Advanced Industrial Science and Technology (AIST), Higashi 1-1, Tsukuba, Ibaraki 305-8565, Japan

Shenggang Li and Dong-Sheng Yang*

Department of Chemistry, University of Kentucky, Lexington, Kentucky 40506

Received: January 11, 2005; In Final Form: May 9, 2005

The copper–monomethylamine and –dimethylamine complexes were produced in a supersonic jet and examined using single-photon zero kinetic energy (ZEKE) photoelectron spectroscopy and theoretical calculations. The adiabatic ionization potentials (I.P.) of the complexes and vibrational frequencies of the corresponding ions were measured from their ZEKE spectra. The equilibrium geometries, binding energies, and vibrational frequencies of the neutral and ionized complexes were obtained from MP2 and B3LYP calculations. The observed vibrational frequencies of the ionic complexes were well-reproduced by both calculations, whereas the Franck–Condon intensity patterns of the spectra were simulated better by MP2 than B3LYP. The observed I.P. and vibrational frequencies of the Cu–NH_n(CH₃)_{3–n} (*n* = 0–3) complexes were compared, and methyl substitution effects on their ZEKE spectra were discussed.

Introduction

Interaction between a copper atom/ion and an ammonia molecule is among the most extensively studied gas phase metal–molecule interactions. Copper–ammonia binding energies have been experimentally measured using high-pressure mass spectrometry,^{1,2} collision induced dissociation,³ reaction kinetics,⁴ and photodissociation spectroscopy.⁴ Infrared⁵ and electron spin resonance⁶ spectroscopies have been used to probe copper–ammonia complexes isolated in Ar matrices. Recently, we have observed the zero kinetic energy (ZEKE) photoelectron spectra of the CuNH₃ and CuND₃ complexes,⁷ which revealed their ionization potentials (I.P.) and vibrational structures in the ionized complexes. There have also been a large number of theoretical studies on structures, binding energies, and vibrational frequencies of the copper atom/ion–ammonia complexes.^{8–15}

It has been known that substitutions for hydrogen atoms in ammonia with an alkyl group greatly influence its interaction with copper ions. Binding energies of a copper ion with mono- (*n*-propyl)amine is stronger than that with ammonia.² At room temperature, a copper ion forms an adduct with an ammonia molecule, which has a lifetime of ~ns and is stabilized by three-body collisions.^{16,17} On the other hand, mono-, di-, and tri-methylamines show fast bimolecular reactions that produce copper hydride and imine ions.¹⁸ Methyl substitutions for hydrogen atoms in ammonia affect the vibronic spectra of metal–ammonia complexes as well. The sequential methyl substitution effects on the M–NH_n(CH₃)_{3–n} (M = Al, Ga, In; *n* = 0–3) complexes have been systematically investigated through measurements of their ZEKE spectra by Yang and co-workers, and striking differences in the vibrational structures of these ion complexes have been found.^{19–21} The fully methyl-substituted complex of CuNH₃, Cu–N(CH₃)₃, has also been

investigated and compared with the Cu–P(CH₃)₃ and Cu–As(CH₃)₃ complexes.^{22,23}

In this paper, we extend the ZEKE study to the Cu complexes of mono- and di-methylamines to systematically examine the methyl substitution effects in the Cu–NH_n(CH₃)_{3–n} series. In addition, theoretical calculations on the Cu–NH₂CH₃ and Cu–NH(CH₃)₂ complexes are performed to compare with the experimental measurements. The trend of the ionization and binding energies and differences in the vibrational structures of the Cu–NH_n(CH₃)_{3–n} complexes are discussed based on experimental and theoretical results.

Experimental and Computational Details

The experimental setup has been described in a previous publication,⁷ and the experimental methods are described next. The copper–methylamine complexes were prepared by reactions of laser-vaporized Cu atoms with the molecular ligands and cooled in a supersonic jet. To produce Cu atoms, a copper rod was vaporized with the second harmonic of a Nd:YAG laser (532 nm, ~2 mJ, Continuum, Surelite I). Monomethylamine (Matheson, 99.5%) or dimethylamine (Matheson, 99.5%) was mixed with helium at a concentration of ~5% and expanded to the vaporization region through a pulsed valve (General Valve 9-279-900) at a stagnation pressure of 3 atm. To locate the ionization thresholds of the complexes, photoionization efficiency (PIE) spectra were taken by recording the ion signal of the complexes as a function of laser wavelength. Masses of the complexes were measured by using a time-of-flight mass spectrometer. ZEKE electrons were produced by first photo-exciting molecules to high-lying Rydberg levels and then ionizing these Rydberg molecules with a pulsed electric field (2 V/cm, 500 ns) delayed (3 μs) from the laser excitation. The photoionization and photoexcitation light was provided by a frequency-doubled dye laser (LambdaPhysik, Scanmate 2) pumped by a XeCl excimer laser (LambdaPhysik, COM-

* Corresponding authors. E-mail: (J.M.) j.miyawaki@aist.go.jp and (D.-S.Y.) dyang0@uky.edu.

TABLE 1: Equilibrium Bond Lengths (Å), Bond Angles (deg), and Vibrational Frequencies (cm⁻¹) of the Cu–NH₂CH₃ and Cu–NH(CH₃)₂ Complexes Calculated at MP2/6-311+G(d,p) Level^a

			Cu–NH ₂ CH ₃		
Ion ¹ A'	length		CuN = 1.931; NH = 1.022; NC = 1.502; CH = 1.091, 1.089, 1.089		
	angle		CuNH = 109.5; CuNC = 116.7; HNH = 104.2; HNC = 108.2; NCH = 110.3, 109.0; HCH = 109.5, 109.5		
	frequency		a': 3488, 3214, 3112, 1639, 1526, 1487, 1305, 1097, 1009, 450, 208 a'': 3553, 3228, 1536, 1359, 1043, 645, 222		
Neutral ² A'	length		CuN = 2.033; NH = 1.019; NC = 1.483; CH = 1.094, 1.090, 1.090		
	angle		CuNH = 108.2; CuNC = 115.8; HNH = 105.5; HNC = 109.3; NCH = 112.4, 108.8; HCH = 109.3, 108.8		
	frequency		a': 3501, 3176, 3083, 1637, 1523, 1476, 1237, 1049, 1014, 315, 166 a'': 3585, 3205, 1533, 1354, 1006, 522, 199		
			Cu–NH(CH ₃) ₂		
Ion ¹ A'	length		CuN = 1.929; NH = 1.022; NC = 1.497; CH = 1.091, 1.091, 1.094		
	angle		CuNH = 107.1; CuNC = 113.4; CNC = 110.1; CNH = 106.1; NCH = 109.0, 109.7, 109.7; HCH = 109.7, 109.1, 109.6		
	frequency		a': 3498, 3212, 3188, 3089, 1537, 1527, 1491, 1311, 1260, 1082, 912, 483, 392, 281, 224 a'': 3213, 3190, 3091, 1524, 1509, 1467, 1439, 1156, 1074, 1038, 231, 192		
Neutral ² A'	length		CuN = 2.043; NH = 1.019; NC = 1.477; CH = 1.092, 1.091, 1.098		
	angle		CuNH = 105.1; CuNC = 112.7; CNC = 110.8; CNH = 107.5; NCH = 108.7, 109.4, 111.5; HCH = 108.6, 108.9, 109.6		
	frequency		a': 3520, 3192, 3152, 3052, 1532, 1522, 1482, 1285, 1241, 988, 921, 416, 345, 243, 178 a'': 3193, 3154, 3053, 1523, 1506, 1463, 1453, 1169, 1100, 1044, 231, 162		

^a B3LYP/6-311+G(d,p): Cu⁺/Cu–N = 1.957/2.117 and 1.961/2.143 Å for Cu–NH₂CH₃ and Cu–NH(CH₃)₂, respectively.

PEX100). Laser wavelengths were calibrated against copper atom transitions.²⁴ The electric field for the ZEKE experiment was generated by a delay pulse generator (Stanford DG535). The ion and ZEKE signals were detected by a dual microchannel plate detector (Hamamatsu, F4655), amplified by a preamplifier (NF, BX-31A), averaged by a gated integrator (Stanford SR250), and stored in a laboratory computer through an A/D converter.

Equilibrium geometries and vibrational frequencies of the complexes were calculated using the Gaussian 98 program package.²⁵ Møller–Plesset second-order perturbation theory (MP2) and density functional theory with Becke's three-parameter hybrid functional using the Lee, Yang, and Parr correlational functional (B3LYP) were used with the 6-311+G(d,p) basis set. Franck–Condon (FC) factors were computed from the theoretical equilibrium geometries, harmonic frequencies, and normal coordinates of the neutral and ion.^{19–23} The Duschinsky effect was considered to account for normal mode differences between the neutral and the ionic molecules in the FC calculations.²⁶ Spectral broadening was simulated by giving each line a Lorentzian line shape with the line width of the experimental spectra.

Results and Discussion

Computation. Table 1 lists the electronic states, equilibrium geometries, and vibrational frequencies of the neutral and ionic Cu–NH₂CH₃ and Cu–NH(CH₃)₂ complexes calculated with the MP2/6-311+G(d,p) method. Results of the B3LYP/6-311+G(d,p) calculations are similar to those of MP2, and only Cu–N bond lengths are listed in the footnote of Table 1. In the following, the MP2 results are discussed unless otherwise noted.

Both complexes have C_s symmetry in their ionic and neutral states, where Cu⁺/Cu is bound to the nitrogen in the methylamines. The neutral ground electronic states of these complexes (²A') are formed by the interaction between ground states of Cu (²S) and methylamines (¹A'). The Cu–N bond length of Cu–NH₂CH₃ and Cu–NH(CH₃)₂ are predicted to be 2.033 and 2.043 Å, and their dissociation energies are 11.60 and 12.02 kcal/mol, respectively. The geometries of the free ligands are slightly affected upon complexation. Compared to the free ligands, the NC and NH bond lengths are increased by 0.018 and 0.005 Å for Cu–NH₂CH₃ and 0.019 and 0.005 Å for Cu–NH(CH₃)₂. The CNH and HNH bond angles of Cu–NH₂CH₃ are decreased by 1.09 and 1.26°, and the CNH and CNC angles of Cu–NH(CH₃)₂ are decreased by 1.68 and 0.99°, respectively.

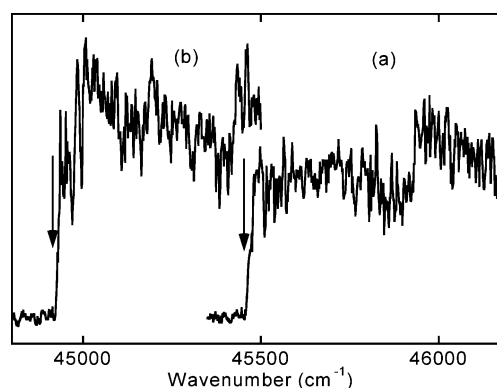


Figure 1. PIE spectra of (a) Cu–NH₂CH₃ and (b) Cu–NH(CH₃)₂. The onsets of the ionization signals located at ~45455 cm⁻¹ for Cu–NH₂CH₃ and ~44920 cm⁻¹ for Cu–NH(CH₃)₂ are indicated by arrows. Their ionization potentials are estimated to be ~45512 and ~44977 cm⁻¹, respectively, after taking into account the shift of 57 cm⁻¹ caused by the electric field (87 V/cm).

The ground states of the ionized complexes are ¹A', which correlate to the ground states of Cu⁺ (¹S) and methylamines (¹A'). The Cu⁺–N bond lengths are predicted to be 1.931 Å for Cu–NH₂CH₃ and 1.929 Å for Cu–NH(CH₃)₂, which are about 0.1 Å shorter than those in the neutral species. The shorter Cu⁺–N bond lengths correspond to the larger dissociation energies in the ion complexes, which are calculated as 57.4 and 59.0 kcal/mol for Cu–NH₂CH₃ and Cu–NH(CH₃)₂, respectively. The large increase of the binding energies in the ionic states leads to a significantly lower I.P. of these complexes than that of the Cu atom (7.762 eV).²⁴ The shorter Cu⁺–N bonds and the larger dissociation energies in the ion complexes are apparently due to removal of the Cu 4s electron, which not only depletes the electron repulsion but also enhances the electron donation and adds a charge–dipole interaction. Upon ionization, the NC and NH bond lengths are increased by 0.019 and 0.003 Å for Cu–NH₂CH₃ and by 0.020 and 0.002 Å for Cu–NH(CH₃)₂, respectively. The H–N–C and H–N–H bond angles of Cu–NH₂CH₃ are reduced by 1.1 and 1.3° and the C–N–C and C–N–H angles of Cu–NH(CH₃)₂ by 0.7 and 1.4°, respectively. Consequently, the Cu–N–C and Cu–N–H bond angles of Cu–NH₂CH₃ are increased by 0.85 and 1.26°, and those of Cu–NH(CH₃)₂ are increased by 0.69 and 1.98°.

Photoionization Spectra. Figure 1 presents the PIE spectra of the copper–methylamine complexes. The PIE spectrum of

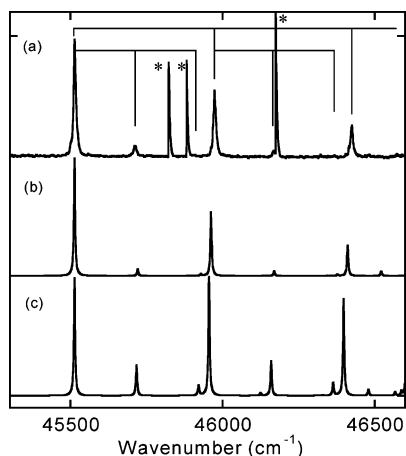


Figure 2. Single-photon ZEKE spectrum of Cu–NH₂CH₃ (a) and its simulations (5 K) calculated with MP2 (b) and B3LYP (c). The peaks with asterisks are due to resonant two-photon ionization of the Cu atom.

Cu–NH₂CH₃ (Figure 1a) displays a sharp onset of the ion signal at ~ 45455 cm⁻¹, as indicated by the arrow. The I.P. of Cu–NH₂CH₃ is estimated to be ~ 45512 cm⁻¹, after the 57 cm⁻¹ correction for the energy shift caused by the electric field applied in the ion extraction region (87 V/cm). In addition, the ion signal shows a stepwise increase beginning at ~ 45910 cm⁻¹. This step at ~ 455 cm⁻¹ above the ionization onset indicates the excitation of the Cu–ligand stretching mode in the ion complex, as observed for other metal–ligand complexes.^{19–23} The PIE spectrum of Cu–NH(CH₃)₂ (Figure 1b) displays the ionization onset at ~ 44920 cm⁻¹, and its I.P. is estimated to be ~ 44977 cm⁻¹. It is, however, difficult to find clear stepwise structures above the ionization threshold to deduce any vibrational frequencies from this PIE spectrum.

ZEKE Spectra. Cu–NH₂CH₃. Figure 2a shows the ZEKE spectrum of Cu–NH₂CH₃. The origin band is observed at 45514(3) cm⁻¹, consistent with the PIE spectrum. From this position, the I.P. of the complex is determined as 5.643(1) eV by taking into account of the I.P. shift caused by the electric field for ionization.⁷ This I.P. is smaller than that of Cu by 2.083 eV, indicating the much larger binding energy in the ionic state than in the neutral state. The I.P. is also smaller than that of CuNH₃ by 950 cm⁻¹, suggesting that methyl substitution of a hydrogen atom of ammonia increases the metal–ligand interaction. The spectrum displays a major progression consisting of three peaks with a spacing of ~ 460 cm⁻¹, which corresponds to the stepwise structure observed in the PIE spectrum. This progression is assigned to the transitions of the Cu⁺–N stretching mode by comparing with the Cu⁺–N stretching frequencies of 470 cm⁻¹ in Cu⁺–NH₃ and theoretical calculations. The MP2/B3LYP frequencies of this mode (ν_{10} , a') are 450/443 cm⁻¹, in good agreement with the measured value. In addition to the major progression, the ZEKE spectrum shows a weak progression with a 199 cm⁻¹ spacing. This frequency matches well with the MP2/B3LYP predicted values of 208/204 cm⁻¹ for the intermolecular bending (Cu⁺–N–C) mode (ν_{11} , a'). The intermolecular bending mode, Cu⁺–N–H or Cu⁺–N–C, was not observed in the ZEKE spectra of Cu–NH₃ (ref 7) and Cu–N(CH₃)₃.²² This is because the metal–ligand bending mode has a double degenerate e symmetry in these C_{3v} symmetry complexes whose $\Delta\nu = 1$ transition is forbidden. The ZEKE spectrum also shows a number of sharp peaks at 45821, 45879, and 46173 cm⁻¹, as marked with asterisks. These peaks arise from resonant two-photon ionization of the copper atom.⁷

TABLE 2: Observed ZEKE Band Positions (cm⁻¹)^a and Assignments for Cu–NH₂CH₃ and Cu–NH(CH₃)₂

Cu–NH ₂ CH ₃		Cu–NH(CH ₃) ₂	
position	assignment	position	assignment
45511	0 ₀ ⁰	44916	Cu
45710	11 ₀ ¹	44976	0 ₀ ⁰
45821	Cu	45186	15 ₀ ¹
45879	Cu	45239	14 ₀ ¹
45907	11 ₀ ²	45361	13 ₀ ¹
45972	10 ₀ ¹	45393	15 ₀ ²
46165	10 ₀ ¹ 11 ₀ ¹	45458	12 ₀ ¹
46173	Cu	45498	14 ₀ ²
46422	10 ₀ ²	45662	12 ₀ ¹ 15 ₀ ¹
		45716	12 ₀ ¹ 14 ₀ ¹
		45821	Cu
		45837	12 ₀ ¹ 13 ₀ ¹
		45859	11 ₀ ¹
		45879	Cu
		45937	12 ₀ ²
		45971	12 ₀ ¹ 14 ₀ ²

^a Uncertainty: ± 3 cm⁻¹.

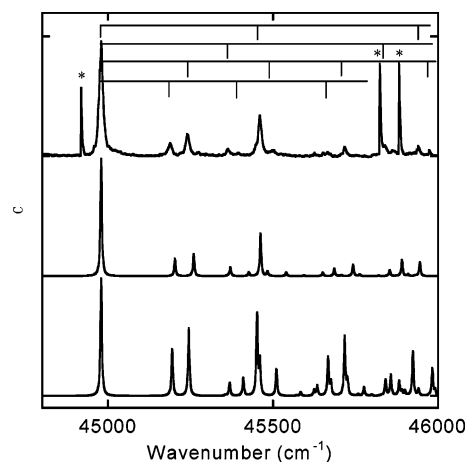


Figure 3. Single-photon ZEKE spectrum of Cu–NH(CH₃)₂ (a) and its simulations (5 K) calculated with MP2 (b) and B3LYP (c). The peaks with asterisks are due to resonant two-photon ionization of the Cu atom.

Figure 2b,c presents simulated spectra from the MP2 and B3LYP calculations. For clarity, the origin bands of these simulations are shifted to the same position as the experimental band. Both simulations show a major Cu⁺–N stretching progression and a weak Cu⁺–N–C bending progression, confirming the previous assignment made by comparing the calculated and measured frequencies. The FC intensities of the two simulated spectra, however, are rather different. The simulation from the MP2 method (Figure 2b) well reproduces the observed intensity pattern. In contrast, the B3LYP simulation (Figure 2c) exhibits longer Cu⁺–N stretching and Cu⁺–N–C progressions. This difference apparently arises from the fact that the differences between the neutral and the ionic equilibrium Cu–N bond lengths and Cu–N–C angles are predicted to be larger by B3LYP than by MP2. In the ZEKE spectrum, no hot bands are observed, and the vibrational temperature of the cluster beam is estimated to be less than 20 K by comparing with the simulations. The observed ZEKE peak positions and assignments for the complex are listed in Table 2.

Cu–NH(CH₃)₂. The ZEKE spectrum of Cu–NH(CH₃)₂ in Figure 3a has its band origin at 44974(3) cm⁻¹, consistent with

TABLE 3: Ionization Potential (I.P.) and Binding Energies (D_0/D_0^+) of $\text{Cu-NH}_n(\text{CH}_3)_{3-n}$ Complexes

	Cu-NH_3^a	$\text{Cu-NH}_2\text{CH}_3$	$\text{Cu-NH}(\text{CH}_3)_2$	$\text{Cu-N}(\text{CH}_3)_3^b$
	ZEKE			
I.P. (eV)	5.761	5.643	5.576	5.546
$\Delta\text{I.P. (eV)}^c$	1.965	2.083	2.150	2.180
	MP2/B3LYP			
I.P. (eV)	5.37/5.95	5.27/5.81	5.21/5.73	5.20/5.69
D_0^+ (kcal/mol)	53.9/57.3	57.4/61.0	59.0/62.1	59.3/61.7
D_0 (kcal/mol)	10.5/9.1	11.6/9.5	12.0/8.9	12.0/7.7
$\Delta\text{I.P. (eV)}^d$	1.88/2.09	1.99/2.23	2.04/2.31	2.06/2.35

^a Ref 7. ^b Ref 22. ^c Difference from I.P.(Cu) = 7.726 eV. ^d $\Delta\text{I.P.} = \text{I.P.}(\text{Cu}) - \text{I.P.}(\text{Cu-L}) = D_0^+(\text{Cu-L}) - D_0(\text{Cu-L})$.

the PIE spectrum and providing the I.P. of 5.576(1) eV. The vibrational structure of $\text{Cu-NH}(\text{CH}_3)_2$ is more complicated than that of $\text{Cu-NH}_2\text{CH}_3$ as previously observed in the ZEKE spectra of the group 13 metal-amines.^{19–21} But, these transitions can be easily assigned to fundamental, overtone, and combination bands of four vibrational frequencies by comparing with the spectrum of the monomethyl species and the theoretical calculations. The frequencies measured from the ZEKE spectrum are 210 cm^{-1} for the $\text{Cu}^+-\text{N}-\text{C}$ bending (ν_{15}, a'), 263 cm^{-1} CH_3 torsional (ν_{14}, a'), 385 cm^{-1} $\text{C}-\text{N}-\text{C}$ bending (ν_{13}, a'), and 482 cm^{-1} Cu^+-N stretching (ν_{12}, a') modes. The frequencies of these modes predicted by the MP2/B3LYP methods are 224/212, 281/266, 392/389, and 483/472 cm^{-1} , respectively. Again, the calculated frequencies are in good agreement with the observed ones.

As in the case of $\text{Cu-NH}_2\text{CH}_3$, the Franck-Condon pattern of the spectrum is reproduced better with MP2 (Figure 3b) than B3LYP (Figure 3c). The B3LYP calculation again predicts a longer Cu^+-N stretching progression and overestimates the intensities of the other transitions, making the simulated spectrum more congested than the observed one, especially in the higher energy region. These computational differences have also been observed in the previous study of the $\text{Cu-N}(\text{CH}_3)_3$ complex. A peak at 45859 cm^{-1} , which is 883 cm^{-1} from the origin band, is tentatively assigned to the $\text{C}-\text{N}-\text{C}$ stretching mode. The MP2/B3LYP frequencies of this mode (ν_{11}, a') are $912/878\text{ cm}^{-1}$. Sharp peaks at 44916 , 45821 , and 45879 cm^{-1} are also due to Cu two-photon transitions. The ZEKE peak positions and assignments for this complex are listed in Table 2.

Comparison of the $\text{Cu-NH}_{3-n}(\text{CH}_3)_n$ ($n = 0-3$) Complexes: Methylation Effects. Table 3 summarizes the I.P. of the $\text{Cu-NH}_{3-n}(\text{CH}_3)_n$ ($n = 0-3$) complexes measured from the ZEKE spectra observed in the present and previous studies.^{7,22} The I.P. and binding energies obtained from MP2/B3LYP calculations are also listed. The I.P. of the Cu atom (7.726 eV) is reduced by 1.965 eV upon the attachment of an ammonia molecule. The I.P. of Cu-NH_3 is further shifted to lower values by sequential methyl substitutions of the hydrogen atoms; however, the I.P. difference between $\text{Cu-NH}_n(\text{CH}_3)_{3-n}$ and $\text{Cu-NH}_{n-1}(\text{CH}_3)_{4-n}$ decreases monotonically (i.e., 0.118, 0.067, and 0.030 eV) from $n = 3-1$. Both MP2 and B3LYP calculations reproduce the trend of I.P., although MP2 underestimates the I.P. values by $\sim 6\%$, whereas B3LYP overestimates them by $\sim 3\%$.

The calculated binding energies of the neutral and ion complexes are evidently increased by the first methyl substitution but not so clear with the second and third substitutions. For example, the binding energies of $\text{Cu-NH}_n(\text{CH}_3)_{3-n}$ calculated at the MP2 level are in the order of $\text{Cu-NH}_3 < \text{Cu-NH}_2\text{CH}_3 < \text{Cu-NH}(\text{CH}_3)_2 \sim \text{Cu-N}(\text{CH}_3)_3$ for both neutral and

ion. On the other hand, the binding energy of $\text{Cu}^+-\text{N}(\text{CH}_3)_3$ is predicted to be smaller than that of $\text{Cu}^+-\text{NH}(\text{CH}_3)_2$ by the B3LYP calculations. For the neutral complexes, B3LYP predicts smaller binding energies for $\text{Cu-NH}(\text{CH}_3)_2$ and $\text{Cu-N}(\text{CH}_3)_3$ than for CuNH_2CH_3 . Similar results have also been reported for the $\text{Ag}^+\text{NH}_{3-n}(\text{CH}_3)_n$ complexes by Reimers and co-workers,²⁷ where the calculations were carried out by the B3LYP method with larger basis sets and corrections of basis set superposition errors. Although methyl substitutions increase the Ag^+ -amine interactions for the first two methyl groups, the binding energy of $\text{Ag}^+-\text{N}(\text{CH}_3)_3$ was slightly smaller than that of $\text{Ag}^+-\text{NH}(\text{CH}_3)_2$.

As has been discussed in previous studies,^{7–15} there are several factors determining the strength of copper-ammonia bonding. One of these is the σ -donation from the nitrogen lone pair to the copper atom. Since the methylation increases σ -donation ability of the ligand amines, the metal-amine interaction is expected to become larger on methylation. We have attempted to evaluate the methylation effect on the dative electron donation by calculating the charges on the Cu atom. However, no clear trend was found from the MP2 and B3LYP calculations on the successive substitution. The second factor is the polarization interaction between metal and ligand. The increasing polarizabilities of the amines on methylation increase the dispersion forces, making the metal-ligand binding stronger. In the ion complexes, additional charge-dipole interactions further stabilize the complexes, but this may have an opposite effect to polarization interaction since dipole moments decrease in the order of $\text{NH}_3 > \text{NH}_2\text{CH}_3 > \text{NH}(\text{CH}_3)_2 > \text{N}(\text{CH}_3)_3$. Furthermore, the Pauli repulsion also affects the metal-molecule bonding. This repulsion may decrease with the methyl substitutions since the $\text{Cu}-\text{N}$ distance is calculated to be lengthened from ammonia to mono-, di-, and tri-methylamine complexes. Overall, the copper-amine binding strengths are determined on a balance of such attractive and repulsive interactions, and sophisticated calculations are required to establish a definitive trend in the binding energies of the three methylamine complexes.

Although the binding energies of the ion and neutral complexes cannot be deduced from the ZEKE spectrum, their difference can be obtained from the observed I.P. shift from the Cu atom to the complex by following the thermochemical relation, $\text{I.P.}(\text{Cu}) - \text{I.P.}(\text{Cu-L}) = D_0^+(\text{Cu}^+-\text{L}) - D_0(\text{Cu-L})$, where D_0^+ and D_0 are bond dissociation energies of the ionic and neutral complexes. The measured $\Delta\text{I.P.}$ values (Table 3) increase with succeeding methyl substitutions, indicating that the methylation has a stronger effect on the ion than on the neutral species. Also, a comparison of the experimental and theoretical values shows that both the MP2 and B3LYP calculations reproduce the I.P. shifts within an error of $\sim 6\%$.

Table 4 summarizes the vibrational frequencies of the $\text{Cu-NH}_n(\text{CH}_3)_{3-n}$ ($n = 0-3$) complexes observed from the ZEKE spectra and MP2/B3LYP/6-311+G(d,p) calculations. The vibrational frequencies obtained from both calculations are generally in good agreement with observations. However, subtle differences are noted between the two computational methods. Frequencies obtained from the MP2 calculation are larger than those from B3LYP for all modes. For the Cu^+-N stretching mode, the experimental and theoretical differences become smaller with increasing molecular sizes, and the MP2 predictions are superior to B3LYP. Especially, MP2 predicts excellent Cu^+-N stretching frequencies for $\text{Cu-NH}(\text{CH}_3)_2$ and $\text{Cu-N}(\text{CH}_3)_3$. For other observed modes, on the other hand, the B3LYP values are better.

TABLE 4: Observed Vibrational Frequencies (cm⁻¹) of the Copper–Methylamine Ions^a

	Cu–NH ₃ ^b	Cu–NH ₂ (CH ₃)	Cu–NH(CH ₃) ₂	Cu–N(CH ₃) ₃ ^c
Cu ⁺ –N–C(H) bend		210 (224/212)	199 (208/204)	
CH ₃ torsion			263 (281/266)	
C–N–C bend			385 (391/389)	
Cu ⁺ –N stretch	470 (451/450)	461 (451/443)	482 (483/472)	268 (270/263)

^a Values in parentheses are obtained from the MP2/B3LYP calculations with the 6-311+G(d,p) basis. ^b Ref 7. ^c Ref 22.

Finally, all of the ZEKE spectra of the Cu–NH_n(CH₃)_{3–n} complexes show a predominant Cu⁺–N stretching progression, which is consistent with a larger change predicted for the Cu–N distance than the other geometric parameters upon ionization. Compared with Cu–NH₃ and Cu–N(CH₃)₂, the spectra of Cu–NH₂CH₃ and Cu–NH(CH₃)₂ show additional transitions involving metal–ligand bending or low-frequency ligand skeleton motions. These additional normal modes become active because of the lower symmetry of the monomethylamine and dimethylamine complexes.

Summary

The neutral copper atom forms stable weakly bound adducts with methylamines. The accurate I.P. of the Cu–NH₂CH₃ and Cu–NH(CH₃)₂ complexes and vibrational frequencies of the corresponding ions were measured from their ZEKE spectra and compared with those of previously studied Cu–NH₃ and Cu–N(CH₃)₃ complexes. The I.P. trend in the Cu–NH_n(CH₃)_{3–n} complexes indicates that the effect of ammonia methylation on the metal–ligand interaction is the most significant for the first methyl substitution and then gradually reduced with further replacement. The binding energies of the neutral and ion complexes obtained from the theoretical calculations are consistent with this observation. The ZEKE spectra of Cu–NH₂CH₃ and Cu–NH(CH₃)₂ display more vibronic transitions than CuNH₃ and Cu–N(CH₃)₃ as a result of lower molecular symmetry. Both MP2 and B3LYP calculations reproduced relatively well the frequencies of the observed vibrational modes; however, the MP2 method yields better FC intensities than B3LYP.

Acknowledgment. D.S.Y. is grateful for financial support from the National Science Foundation and the donors of the Petroleum Research Fund of the American Chemical Society.

References and Notes

(1) Holland, P. M.; Castleman, A. W., Jr. *J. Chem. Phys.* **1982**, *76*, 4195.

- (2) Deng, H.; Kebarle, P. *J. Am. Chem. Soc.* **1998**, *120*, 2925.
 (3) Walter, D.; Armentrout, P. B. *J. Am. Chem. Soc.* **1998**, *120*, 3176.
 (4) Mitchell, S. A.; Lian, L.; Rayner, D. M.; Hackett, P. A. *J. Phys. Chem.* **1996**, *100*, 15708.
 (5) Ball, D. W.; Hauge, R. H.; Margrave, J. L. *Inorg. Chem.* **1989**, *162*, 123.
 (6) Doan, V.; Kasai, P. H. *J. Phys. Chem. A* **1997**, *101*, 8115.
 (7) Miyawaki, J.; Sugawara, K. *J. Chem. Phys.* **2003**, *119*, 6539.
 (8) Bauschlicher, C. W.; Langhoff, S. R.; Partridge, H. *J. Chem. Phys.* **1991**, *94*, 2068.
 (9) El-Nahas, A. M.; Tajima, N.; Hirao, K. *J. Mol. Struct. (THEOCHEM)* **1999**, *469*, 201. El-Nahas, A. M.; Hirao, K. *J. Phys. Chem. A* **2000**, *104*, 138.
 (10) Simon, J. A.; Palke, W. E.; Ford, P. C. *Inorg. Chem.* **1996**, *35*, 6413.
 (11) Hoyau, S.; Ohanessian, G. *Chem. Phys. Lett.* **1997**, *280*, 266.
 (12) Luna, A.; Amekraz, B.; Tortajada, J. *Chem. Phys. Lett.* **1997**, *266*, 31. Luna, A.; Alcamí, M.; M^o, O.; Yáñez, M. *Chem. Phys. Lett.* **2000**, *320*, 129. Luna, A.; Alcamí, M.; M^o, O.; Yáñez, M. *Int. J. Mass Spectrom.* **2000**, *210*, 215.
 (13) Chen, W.-T.; Fournier, R. *Chem. Phys. Lett.* **1999**, *315*, 257. Fournier, R. *J. Chem. Phys.* **1995**, *102*, 5396.
 (14) Papai, I. *J. Chem. Phys.* **1995**, *103*, 1860.
 (15) Antusek, A.; Urban, M.; Sadlej, A. J. *J. Chem. Phys.* **2003**, *119*, 7247.
 (16) Castleman, A. W., Jr.; Weil, K. G.; Sigsworth, S. W.; Leuchtner, R. E.; Keese, R. G. *J. Chem. Phys.* **1987**, *86*, 3829.
 (17) Clemmer, D. E.; Armentrout, P. B. *J. Phys. Chem.* **1991**, *95*, 3084.
 (18) Sigsworth, S. W.; Castleman, A. W., Jr. *J. Am. Chem. Soc.* **1989**, *111*, 3566.
 (19) Li, S.; Rothschofs, G. K.; Fuller, J. F.; Yang, D.-S. *J. Chem. Phys.* **2003**, *118*, 8636.
 (20) Li, S.; Fuller, J. F.; Sohnlein, B. R.; Yang, D.-S. *J. Chem. Phys.* **2003**, *119*, 8882.
 (21) Rothschofs, G. K.; Li, S.; Perkins, J. S.; Yang, D.-S. *J. Chem. Phys.* **2001**, *115*, 4565.
 (22) Li, S.; Sohnlein, B. R.; Rothschofs, G. K.; Fuller, J. F.; Yang, D.-S. *J. Chem. Phys.* **2003**, *119*, 5406.
 (23) Fuller, J. F.; Li, S.; Sohnlein, B. R.; Rothschofs, G. K.; Yang, D.-S. *Chem. Phys. Lett.* **2002**, *366*, 141.
 (24) Moore, C. E. *Atomic Energy Levels, National Standards Reference Data, Series No. 35*; National Bureau of Standards: Washington, DC, 1971.
 (25) *Gaussian 98 (Revision A.11)*; Gaussian, Inc.: Pittsburgh, PA, 2001.
 (26) Duschinsky, F. *Acta Physicochim.* **1937**, *URSS* *7*, 551.
 (27) Widmer-Cooper, A. N.; Lindoy, L. F.; Reimers, J. R. *J. Phys. Chem. A* **2001**, *105*, 6567.